Saliba, N. G. and Gardner , L. (2018). Deformation-based design of stainless steel cross-sections in shear. Thin-Walled Structures. **123**, 324-332.

Deformation-based design of stainless steel cross-sections in shear

N. G. Saliba[1] and L. Gardner[2]

[1]*University of Balamand, Lebanon*

[2]*Imperial College London, UK*

Abstract

The continuous strength method (CSM) is a recently developed deformation-based design method for metallic structures. In this method, cross-section classification is replaced by a normalised deformation capacity, which defines the maximum strain that a cross-section can endure prior to failure. This limiting strain is used in conjunction with an elastic, linear-hardening material stress-strain model to determine cross-section capacity allowing for the influence of strain hardening. To date, the CSM has been developed for the determination of cross-section capacity under normal stresses (i.e. compression, bending and combined loading), where it has been shown to offer more accurate predictions than current codified methods. In this paper, extension of the CSM to the determination of shear resistance is described. The relationship between the normalized shear deformation capacity, referred to as the shear strain ratio, and the web slenderness is first established on the basis of experimental and numerical data. The material model and proposed resistance functions are then described. Comparisons of the developed method with the ultimate shear capacity of a series of tested stainless steel plate girders show that improved resistance predictions of test capacity over current design methods are achieved.

Keywords: Continuous strength method, Deformation capacity, Plate girder, Shear buckling, Stainless steel, Strain hardening, Web slenderness.

1. Introduction

The current codified approach for the calculation of the compression, bending and shear resistances of stainless steel cross-sections has been observed throughout published studies [1-6] to be conservative in the cases of elements of low slenderness. This may be attributed to: (1) the assignment of cross-sections to discrete behavioural classes and (2) assuming the maximum attainable stress is the 0.2% proof stress f_y (i.e. an elastic, perfectly plastic approximation to the material stress-strain curve and ignoring strain hardening). With initial cost and hence design efficiency being of paramount importance in the selection of stainless steel for main structural components, the application of more sophisticated design methods, exploiting the true material behaviour, such as the continuous strength method (CSM), is considered to be warranted.

Following the successful application of the CSM to stainless steel cross-sections under compression, bending and combined loading [1-6], this paper presents developments of the method towards its extension to the calculation of shear resistance. A review of the key components of the CSM is first presented. Test and numerical data collected from Saliba and Gardner [7] and Saliba et al. [8] have been utilized to establish the preliminary shear base curve and subsequently the CSM shear design equations. The effect of applying the CSM to estimate the shear resistance and bending resistance of plate girders has been evaluated considering two scenarios: (1) the web contribution to the shear resistance calculated according to the EN 1993-1-4 [8, 9] design equations but the flange contribution and the bending resistance of the cross-section calculated with allowance for strain hardening according to the CSM and (2) both web and flange contributions to the shear resistance determined using the CSM for shear presented herein and the bending resistance also calculated according to the CSM.

2. Literature review

Initial research into the shear resistance of slender plate girders, carried out by Bleich [10] and later by Basler et al. [11, 12], assumed that a theoretical tension field extending over the whole depth of the web is formed once shear buckling occurs. The shear resistance of plate girders was considered accordingly as the sum of the buckling and postbuckling resistances of the web only, ignoring the flange contribution. This approach was found by Calladine [13] and Porter et al. [14] to be conservative, and was developed further by Rockey et al. [15, 16] to improve its accuracy, though shortcomings remained for the case of plate girders with widely spaced transverse web stiffeners.

ENV 1993-1-1 (1992) [17] allowed the calculation of shear resistance for carbon steel plate girders using either the tension field method or the simple post critical method [18], though these two methods were replaced [19-21] by improved design equations in the final EN standard. The current design equations for shear buckling for carbon steel sections, included in EN 1993-1-5 [22], are based on the rotated stress field method developed by Höglund [19, 23, 24]. The rotated stress field method accounts for the postbuckling shear strength of both unstiffened and stiffened webs and takes into consideration the flange contribution.

In EN 1993-1-5 [22], the ultimate shear resistance $V_{b,Rd}$ is defined as the sum of the web shear buckling resistance $V_{bw,Rd}$ and the flange contribution $V_{bf,Rd}$ as given in Eq. (1).

$$V_{b,Rd}=V_{bw,Rd}+V_{bf,Rd}\leq\frac{\eta f_{yw}h_w t_w}{\sqrt{3}\gamma_{M1}} \tag{1}$$

where the influence of strain hardening is considered through the parameter η, h_w is the web depth, t_w is the web thickness, f_{yw} is the yield strength of the web, and γ_{M1} is a partial safety factor.

The web contribution $V_{bw,Rd}$ is given by Eq. (2):

$$V_{bw,Rd}=\frac{\chi_w f_{yw}h_w t_w}{\sqrt{3}\gamma_{M1}} \tag{2}$$

where χ_w is the web shear buckling reduction factor.

The flange contribution $V_{bf,Rd}$ is defined by Eq. (3):

$$V_{bf,Rd}=\left(\frac{b_f t_f^2 f_{yf}}{c\gamma_{M1}}\right)\left(1-\left(\frac{M_{Ed}}{M_{f,Rd}}\right)^2\right) \tag{3}$$

in which b_f is the overall flange width, t_f is the flange thickness, f_{yf} is the yield strength of the flange, M_{Ed} is the coexistent design bending moment, $M_{f,Rd}$ is the moment resistance of the flanges alone and finally, the longitudinal distance of the plastic hinges that form in the flanges from the transverse stiffeners, c, is given by Eq. (4):

$$c=\left(0.25+\frac{1.6b_f t_f^2 f_{yf}}{t_w h_w^2 f_{yw}}\right)a \qquad (4)$$

where a is the distance between the transverse stiffeners.

The interaction between shear and bending moment commonly arises in practice and has been the subject of numerous studies [10, 11, 25-29]. EN 1993-1-5 (2006) [22] prescribes a reduced bending resistance when the coexistent shear force exceed 50% of the shear resistance.

For stainless steel, the first codified shear resistance design equations were presented in the prestandard ENV 1993-1-4 (1996) [30]. The equations were developed on the basis of an experimental study carried out by Carvalho et al. [31] and the simple post critical method of ENV 1993-1-1 (1992) [17], with adjustments to account for the particular nonlinear material characteristics of stainless steel. These equations were later shown by Olsson [32] to be conservative and revised equations were included in the final EN standard, EN 1993-1-4 (2006) [33]. The improved shear design equations were based on the rotated stress field method and are of similar form to those given in EN 1993-1-5 (2006) [22], but with modified functions for the shear buckling reduction factor χ_w, no differentiation between rigid and non-rigid end posts, and an alternative definition of the distance c, as given in Eq. (5).

$$c=\left(0.17+\frac{3.5b_f t_f^2 f_{yf}}{t_w h_w^2 f_{yw}}\right)a \ \text{ with } \ \frac{c}{a}\leq 0.65 \qquad (5)$$

Further improvements to the design rules were proposed in [34-36] and most recently by Saliba et al. [8], who considered an enlarged pool of experimental data and introduced a distinction between web panels with rigid and non-rigid end posts. These proposed equations are presented in Table 1, and, following a recent amendment, are now incorporated into EN 1993-1-4:2006+A1:2015 [9].

3. The CSM for the determination of compression and bending resistances

3.1 Overview

The continuous strength method (CSM) [1] is a recently developed method which offers an alternative approach to calculating the resistance of metallic cross-sections. Contrary to the traditional approach which assumes elastic, perfectly plastic material behaviour, the CSM allows exploitation of material strain hardening, such as that exhibited by stainless steel and aluminium. The CSM considers local buckling in the elastic or inelastic range and the associated limiting strain to be the key physical restriction to the exploitation of the spread of plasticity and strain hardening of the material. Hence, the maximum attainable failure stress of a stainless steel cross-section is considered as a continuous function of the material properties, the geometry of the cross-section and the imposed loading, rather than simply a material specific stress (i.e. the yield stress).

The CSM deviates from traditional cross-section classification by adopting a continuous relationship between cross-sectional slenderness and deformation capacity. The deformation capacity of the cross-section is determined from an experimentally derived 'base curve' which links the limiting strain at failure due to local buckling ε_{csm} to the cross-section slenderness [1]. The stress corresponding to this limiting failure strain, is then determined from the material model, which incorporates strain hardening.

A detailed description of the development of the CSM and its successful application to stainless steel, aluminium alloys, high strength steel and carbon steel is presented in [1, 38-40], while the most recent developments and improvements to the method are presented in Gardner et al. [3], Afshan and Gardner [6] and Zhao et al. [41].

3.2 Deformation capacity

The local cross-section slenderness is defined in the CSM through Eq. (6):

$$\bar{\lambda}_p=\sqrt{\frac{f_y}{\sigma_{cr}}} \tag{6}$$

where f_y is the material yield (0.2% proof) stress and σ_{cr} is the elastic buckling stress of the full cross-section as used in the direct strength method (DSM) [42], or conservatively, of the most slender constituent plate element.

The deformation capacity $\varepsilon_{csm}/\varepsilon_y$, according to the CSM, is defined by the base curve, given by Eqs. (7) and (8) for non-slender ($\bar{\lambda}_p \leq 0.68$) and slender ($\bar{\lambda}_p > 0.68$) cross-sections, respectively [6, 41]:

$$\frac{\varepsilon_{csm}}{\varepsilon_y}=\frac{0.25}{\bar{\lambda}_p^{3.6}} \quad \text{but } \frac{\varepsilon_{csm}}{\varepsilon_y} \leq \min\left(15, \frac{C_1\varepsilon_u}{\varepsilon_y}\right) \text{ for } \bar{\lambda}_p \leq 0.68 \tag{7}$$

$$\frac{\varepsilon_{csm}}{\varepsilon_y}=\left(1-\frac{0.222}{\bar{\lambda}_p^{1.050}}\right)\left(\frac{1}{\bar{\lambda}_p^{1.050}}\right) \text{ for } \bar{\lambda}_p > 0.68 \tag{8}$$

where $\varepsilon_y = f_y/E$ is the yield strain of the material, E is the Young's modulus, ε_{csm} is the CSM limiting strain for the cross-section, and ε_u is the strain at the ultimate tensile stress, which can be approximated from $\varepsilon_u = C_3(1 - f_y/f_u)$; C_1 and C_3 are material parameters taken as $C_1 = 0.10$ and $C_3 = 1.0$ for austenitic and duplex stainless steel and $C_1 = 0.40$ and $C_3 = 0.60$ for ferritic stainless steel.

3.3 Material model and cross-section resistance

An elastic, linear hardening material model, as depicted in Fig. 1, is adopted in the CSM with the relationship between stress σ_{csm} and strain ε_{csm} defined by Eq. (9):

$$\left.\begin{aligned} &\sigma_{csm}=E\varepsilon_{csm} && \text{for } \frac{\varepsilon_{csm}}{\varepsilon_y}\leq 1 \\ &\sigma_{csm}=f_y+E_{sh}\varepsilon_y\left(\frac{\varepsilon_{csm}}{\varepsilon_y}-1\right) && \text{for } \frac{\varepsilon_{csm}}{\varepsilon_y}>1 \end{aligned}\right\} \tag{9}$$

where E_{sh} is the strain hardening slope, calculated from Eq. (10):

$$E_{sh}=\frac{f_u-f_y}{C_2\varepsilon_u-\varepsilon_y} \tag{10}$$

where f_u is the ultimate tensile stress of the material and C_2 is a material parameter taken equal to 0.16 for austenitic and duplex stainless steel and 0.45 for ferritic stainless steel.

Finally, having established the strain ratio $\varepsilon_{csm}/\varepsilon_y$ (i.e. the deformation capacity) of the cross-section and the material stress-strain curve, the cross-section compression resistance $N_{csm,Rd}$ and major axis bending resistance $M_{y,csm,Rd}$ are calculated according to Eqs. (11) and (12), respectively [3, 6]:

$$N_{c,Rd}=N_{csm,Rd}=\frac{A\sigma_{csm}}{\gamma_{M0}} \tag{11}$$

$$\left.\begin{aligned} &M_{y,c,Rd}=M_{y,csm,Rd}=\frac{W_{el}\sigma_{csm}}{\gamma_{M0}} && \text{for } \frac{\varepsilon_{csm}}{\varepsilon_y}\leq 1 \\ &M_{y,c,Rd}=M_{y,csm,Rd}=\frac{W_{pl,y}f_y}{\gamma_{M0}}\left[1+\frac{E_{sh}}{E}\frac{W_{el,y}}{W_{pl,y}}\left(\frac{\varepsilon_{csm}}{\varepsilon_y}-1\right)-\left(1-\frac{W_{el,y}}{W_{pl,y}}\right)\bigg/\left(\frac{\varepsilon_{csm}}{\varepsilon_y}\right)^{\alpha}\right] && \text{for } \frac{\varepsilon_{csm}}{\varepsilon_y}>1 \end{aligned}\right\} \tag{12}$$

where A is the gross-cross-sectional area, W_{el} is the elastic section modulus, W_{pl} is the plastic section modulus, α is a parameter dependent on cross-section shape, with $\alpha = 2$ for I-sections in major axis bending and γ_{M0} is the partial safety factor for cross-section resistance, with a recommended value of 1.1 given in EN 1993-1-4 [9].

4. Extension of the CSM to the determination of shear resistance

4.1 Introduction

The CSM currently applies to the calculation of cross-section resistances under normal stresses (i.e. compression, bending and combinations thereof). In this section of the paper, extension of the continuous strength method to include the determination of shear resistance is presented. The approach adopted to develop the CSM shear resistance equations is in harmony with the method described in Section 3.2 of this paper. Underpinning data have been derived from a combination of physical experiments [7] and finite element simulations, with the latter summarized in the following section.

4.2 Finite element simulations

Finite element simulations on stainless steel plate girders were carried out to supplement the existing test results using the general-purpose finite element analysis package ABAQUS [43]. The experimental results reported in Saliba and Gardner [7] were firstly used to validate the models. Subsequently, a parametric study was conducted to cover a wider range of web slendernesses and ratios of shear force to bending moment. The results are used herein to extend the continuous strength method to cover the determination of shear resistance of structural cross-sections.

The finite element (FE) type S4R, a four-noded doubly curved general-purpose shell element with reduced integration and finite membrane strains was adopted throughout the study. This element has six degrees of freedom per node and is suitable for the modelling of a range of shell thicknesses, as demonstrated in previous similar studies [44, 45]. In the validation phase of the numerical study, the measured stress-strain response of the tested plate girders was represented by means of the two-stage Ramberg–Osgood expression [38, 46, 47] and, for incorporation into ABAQUS, a multi-linear arrangement, defined in terms of true stress and log plastic strain, was adopted. The compressive material properties were applied to the upper halves of the FE models whereas the tensile material properties were applied to the lower halves. The loading and boundary conditions adopted in the FE model were selected to duplicate the experimental setup. The load was applied through a bearing plate at the centre of the FE models. The plate was modelled using solid elements and 'shell-to-solid' coupling was used to define for the interaction between the bearing plate and the top flange of the plate girder. A typical FE model is shown in Fig. 2.

The method of analysis was divided into two stages. In the first stage, a linear eigenvalue buckling analysis was carried out to determine the lowest relevant elastic buckling mode. This mode shape, scaled by the imperfection amplitude derived from the Dawson and Walker model [48] as modified by Gardner and Nethercot [37], was adopted as the initial geometric imperfection. Note that although this imperfection amplitude was derived from measurements on cold-formed stainless steel plated sections, it has also been successfully applied and shown to yield accurate results in FE simulations of welded stainless steel plated sections [4, 7]. The second phase was a materially and geometrically nonlinear analysis of the imperfect structure conducted using the modified Riks method [43], an algorithm that enables effective solutions to be found to unstable problems and adequately traces nonlinear unloading paths. Residual stresses were not included in the finite element modelling as their influence on the shear buckling behaviour of lean duplex stainless steel plate girders was found by Saliba and Gardner [4] to be insignificant.

Following validation of the numerical models against experimental results [5], a series of parametric studies were conducted. The aim of the parametric study was to increase the available structural performance data on stainless steel plate girders covering a broader range of web slenderness, web panel aspect ratios and end post conditions. More than forty finite element simulations were performed. A summary of the geometric properties and end post rigidity (r = rigid and nr = non-rigid) of the modelled plate girders is presented in Table 2; a nominal 0.2% proof strength of 450 N/mm^2 was employed for both the flanges and web. The plate girder designation system may be illustrated by means of an example – I-700×200×60×20-0.86-r refers to an I-section plate girder with h_w = 700 mm, b_f = 200 mm, t_f = 60 mm, t_w = 20 mm, a/h_w (i.e. the web panel aspect ratio, where a is the spacing of the transverse web stiffness) = 0.86 and a rigid end post. The numerical results were used, together with the experimental data, to assess the structural behaviour of lean duplex stainless steel plate girders, to examine the applicability of current codified design provisions and to develop the CSM for shear.

4.3 Web slenderness

When considering shear buckling, the web slenderness $\bar{\lambda}_w$ may be determined from Eq. (13):

$$\bar{\lambda}_w = \sqrt{\frac{\tau_y}{\tau_{cr}}} \tag{13}$$

where τ_y is the 0.2% proof strength in shear ($\tau_y = f_{y,w}/\sqrt{3}$, where $f_{y,w}$ is the yield strength of the web) and τ_{cr} is the elastic critical shear buckling stress of the web panel, as set out in EN 1993-1-5 [22]. The elastic shear buckling stress could alternatively be calculated on the basis of the full cross-section, allowing for element interaction [49, 50].

The web yield slenderness limit, defining the transition point between a slender and non-slender web was assumed to be $\bar{\lambda}_w = 0.65$, as set out in EN 1993-1-4 [9]; beyond this point, the influence of strain hardening becomes less relevant to the shear resistance of plate girders. According to EN 1993-1-4 [9], the effect of strain hardening is approximately accounted for by specifying the web shear buckling reduction factor χ_w equal to 1.2 for $\bar{\lambda}_w < 0.54$.

4.4 Shear deformation capacity

4.4.1 Shear strain definition

The shear strain γ arising due to the existence of a shear stress τ may be visualized by referring to Fig. 3 in which a rectangular element of material subject to shearing stresses in one plane is considered. Those shearing stresses distort the rectangular face of the block into a parallelogram. The change of angle due to this distortion is referred to as the (engineering) shear strain γ, and is the total measure of shear strain ($\alpha + \beta$) in the x-y plane, as defined in Fig. 4.

4.4.2 Shear buckling strain

The test and numerical data summarized in [7, 8] have been utilized to determine the shear deformation capacity for plate girders with a range of web slendernesses, and subsequently to derive the CSM shear base curve. This involves finding the shear buckling strain γ_{sb} at the ultimate load of each plate girder and subsequently the CSM shear limiting strain γ_{csm}. Data were derived by three means:

1- Method 1: For the tested duplex stainless steel plate girders described in [7], the shear buckling strain γ_{sb} was found using the measurements of the two diagonal string potentiometers. The calculation of the angles (i.e. shear strain) in both diagonal directions is depicted in Fig. 5.

2- Method 2: For the numerical simulations [7], the shear buckling strain γ_{sb} was found in a similar manner to the above mentioned approach by taking the diagonal measurements directly from ABAQUS [43].

3- Method 3: For data from published studies collected by Saliba et al. [8], the shear strain was obtained by calculating the angle γ_{δ} from the deflection of the plate girder (see Fig. 6). The maximum mid-span in-plane deflection was found from published load-displacement curves. The maximum deflection comprises both bending and shear deformation. The bending displacement can be approximately eliminated by multiplying the total measured vertical deflection (i.e. $\delta_{total,test}$) by a shear deflection factor defined as $\delta_{s,theory}/(\delta_{s,theory} + \delta_{b,theory})$, where $\delta_{s,theory}$ is the theoretical elastic shear deflection and $\delta_{b,theory}$ is the theoretical elastic bending deflection. This approach assumes that the ratio of the displacements due to bending and due to shear remains approximately constant throughout the loading history including into the inelastic regime.

There was generally good consistency between shear strains determined by means of the three methods described above. Results were not available for all specimens using the three methods, but for the available data, the average ratio of shear strains obtained from Method 1 to those of Method 2 was 0.99 (8 specimens); similarly, the average Method 1/ Method 3 ratio was 1.06 (8 specimens) and the average Method 2/ Method 3 ratio was 1.02 (53 specimens).

4.4.3 CSM shear base curve

Having defined the web slenderness and explained the calculation of the shear buckling strain γ_{sb} (i.e. the shear strain at peak load), the corresponding normalized shear deformation capacity of the cross-section γ_{csm}/γ_y, termed the shear strain ratio, and the web slenderness can be derived. The resulting relationship between the two, referred to as the shear base curve is given by Eq. (14) for non-slender sections ($\bar{\lambda}_w \leq 0.65$) and shown in Fig. 7.

$$\frac{\gamma_{csm}}{\gamma_y}=\frac{0.18}{\bar{\lambda}_w^{3.98}} \text{ but } \frac{\gamma_{csm}}{\gamma_y}\leq\min\left(15, \frac{C_1\gamma_u}{\gamma_y}\right) \text{ for } \frac{\gamma_{csm}}{\gamma_y}\geq 1 \tag{14}$$

where $\gamma_y = \tau_y/G$ is the shear yield strain of the material, $\gamma_u=2(1+\nu)\varepsilon_u/\sqrt{3}$ is the ultimate shear strain and ε_u is as previously defined, $G = E/2(1+\upsilon)$ is the shear modulus, υ is Poisson's ratio and γ_{csm} is the CSM limiting shear strain of the section. It may be seen from Eq. (14) that two upper bounds are applied to the limiting strain ratio γ_{csm}/γ_y; these mirror those employed in the CSM under normal stresses. The first limit of 15 is to avoid excessive deformations, while the second limit of $C_1\gamma_u/\gamma_y$ is to avoid overpredictions of material strength from the CSM bi-linear material model.

Eq. (14) was derived as follows: using an analogous approach to [3, 6], the CSM limiting shear strain γ_{csm} for each experiment, was defined as follows:

1- For $\bar{\lambda}_w \leq 0.65$ (i.e. non-slender cross-sections), $\gamma_{csm} = \gamma_{sb} – 0.003$. The value 0.003 was determined by converting the plastic strain at the 0.2% proof stress to a shear plastic strain using the conversion given in Eq. (15).

$$\gamma=\frac{2(1+\nu)\varepsilon}{\sqrt{3}} \tag{15}$$

2- For $\bar{\lambda}_w > 0.65$, and $V_{u,test} \geq V_y$ (where $V_{u,test}$ is the ultimate load in shear and V_y is the yield load in shear), $\gamma_{csm} = \gamma_{sb} – 0.003$.

3- For $\bar{\lambda}_w > 0.65$, and $V_{u,test} < V_y$, the ratio γ_{csm}/γ_y is defined as the ratio of the ultimate load in shear V_u to the yield load in shear V_y (i.e. $\gamma_{csm}/\gamma_y = V_{u,test}/V_y$).

Once the data points for each experiment and numerical model (i.e. $\bar{\lambda}_w$, γ_{csm}/γ_y) were positioned, the shear base curve for non-slender cross-sections (Eq. (14)) was fitted by means of nonlinear least squares regression [51], ensuring that the curve passed through the point ($\bar{\lambda}_w$=0.65, γ_{csm}/γ_y = 1). The scatter of the data is attributed partly to the inherent variability associated with experiments, but may also relate to the different flange geometries between the tested plate girders, which is not accounted for in the traditional measure of web slenderness.

For cross-sections that are slender in shear (i.e. $\bar{\lambda}_w > 0.65$), the limiting CSM strain ratio is simply equal to the ratio of failure load to yield load in shear (i.e. the shear buckling reduction factor χ_w). Adopting the EN 1993-1-4 [9] shear buckling curves, this is therefore given by Eq. (16):

$$\left.\begin{aligned} \frac{\gamma_{csm}}{\gamma_y} &= \chi_w = \frac{1.19}{0.54+\bar{\lambda}_w} && \text{for } \bar{\lambda}_w > 0.65 \text{ and non-rigid endposts} \\ \frac{\gamma_{csm}}{\gamma_y} &= \chi_w = \frac{1.56}{0.91+\bar{\lambda}_w} && \text{for } \bar{\lambda}_w > 0.65 \text{ and rigid endposts} \end{aligned}\right\} \tag{16}$$

4.5 Shear resistance according to the CSM

The elastic, linear hardening material model used for normal stresses described in Section 3.3 (Fig. 1) may be converted into a shear stress-strain model (see Fig. 8) with the initial slope defined by the shear modulus G and the linear hardening region defined by the shear strain hardening modulus $G_{sh} = E_{sh}/2(1+\upsilon)$. Hence, similar to Eq. (9), the CSM limiting shear stress can be calculated from Eq. (17).

$$\left.\begin{aligned} \tau_{csm} &= G\gamma_{csm} && \text{for } \gamma_{csm} < \gamma_y \\ \tau_{csm} &= \tau_y + G_{sh}(\gamma_{csm} - \gamma_y) && \text{for } \gamma_{csm} \geq \gamma_y \end{aligned}\right\} \tag{17}$$

Finally, the web shear resistance $V_{bw,csm,Rd}$ is given by Eq. (18) as the product of the web area $A_w = h_w t_w$ (where h_w is the web depth and t_w is the web thickness) and the limiting shear stress τ_{csm}.

$$V_{bw,csm,Rd} = A_w \tau_{csm} / \gamma_{M1} \tag{18}$$

The flange contribution to the shear resistance following the CSM philosophy $V_{bf,csm,Rd}$ is given by Eq. (19), in which the CSM limiting stress σ_{csm} is used in place of the material yield stress f_{yf}, including in the calculation of the CSM moment capacity of the flanges alone $M_{f,csm,Rd}$.

$$V_{bf,csm,Rd}=\left(\frac{b_f t_f^2 \sigma_{csm}}{c\gamma_{M1}}\right)\left(1-\left(\frac{M_{Ed}}{M_{f,csm,Rd}}\right)^2\right) \tag{19}$$

5. Comparisons between test/FE data and design models

In this section, the continuous strength method is used to predict the resistance of the test data collected from Saliba et al. [8] and the FE data generated by Saliba and Gardner [7] on stainless steel plate girders under combined shear and bending. In applying the CSM, two scenarios have been considered; (1) shear resistance calculated according to EN 1993-1-4 [8, 9] but with the flange contribution calculated according to the CSM (i.e. $V_{b,Rd} = V_{bw,Rd} + V_{bf,csm,Rd}$) and bending resistance calculated according to the CSM (i.e. $M_{csm,Rd}$) and (2) both web and flange contributions to the shear resistance found according to the CSM (i.e. $V_{b,csm,Rd} = V_{bw,csm,Rd} + V_{bf,csm,Rd}$) and also the bending resistance calculated according to the CSM (i.e. $M_{csm,Rd}$). Consideration of the two scenarios enables the benefit that is derived from strain hardening to the bending resistance and the shear resistance to be identified in isolation.

A comparison, assuming proportional loading (i.e. the ratio of shear force to bending moment remains constant) denoted as U (i.e. the utilization ratio), between the ultimate capacity achieved by the test specimens or FE simulations $R_{test,FE}$ and the predicted capacity according to the CSM R_{csm} considering scenarios 1 and 2 is presented in Figs 9 and 10, respectively, in which the predictions of EN 1993-1-4 [8, 9] R_{EC3} are also included. For the CSM, the utilization ratio $U_{csm} = R_{test,FE}/R_{csm}$, while for EC3, the utilization ratio $U_{EC3} = R_{test,FE}/R_{EC3}$, as illustrated in Fig. 11. The numerical comparisons, including the mean and coefficient of variation (COV) of the CSM and EN 1993-1-4 [8, 9] predictions in relation to the test and numerical data are presented in Tables 3 and 4. The comparisons of Fig. 9 and Table 3 show that applying the CSM to calculate both the total shear and bending resistances (i.e. CSM scenario 2) gives the most accurate predictions of the available data. The mean ratio of test to CSM capacity is 1.11 with a coefficient of variation (COV) of 0.10, an enhancement of 5% on average over the EN 1993-1-4 [8, 9] predictions. Furthermore, when considering the comparisons of Fig. 10 and Table 4 (i.e. for plate girder test and FE results for web slenderness $\bar{\lambda}_w < 0.65$) the mean ratio of test to CSM capacity is 1.07 with a coefficient of variation (COV) of 0.04, an improvement of 11% on average over the EN 1993-1-4 [8, 9] predictions. Note that results from Figs 9 and 10 and Tables 3 and 4 show that CSM scenario 1 (i.e. shear resistance calculated according to EN 1993-1-4 [8, 9] but with the flange contribution and bending resistance calculated according to the CSM) also provides worthwhile improvements over the EN 1993-1-4 [8, 9] predictions. A typical example of the enhancement that the CSM offers over EN 1993-1-4 [9] can be seen in Fig. 11 where the moment-shear interaction diagrams of plate girder I-700×200×60×25-0.86 [7] according to both design methods are plotted. Similar results would be anticipated for cross-sections formed from other metallic materials.

6. Conclusions

The importance of developing novel design methods, such as the continuous strength method, that account for the true material behaviour of stainless steel (including the effect of strain-hardening) and subsequently allow for more efficient designs has been discussed. An overview of the development of the continuous strength method to predict the compression and bending resistances of cross-sections has been provided in this paper. Development of the continuous strength method to predict the shear resistance of plate girders has been presented. A base curve for shear, defining the relationship between web slenderness and web shear deformation capacity, along with a suitable linear hardening material model, have been derived. Comparisons of the shear resistance predictions from the developed CSM for shear have been made against the test and numerical data collected in [7, 8]. These comparisons show that applying the CSM to calculate the flange contribution to shear resistance and bending resistance (i.e. CSM scenario 1) provides more accurate results than the codified provisions, while adopting the CSM to predict both the web and flange contributions to shear resistance and the bending resistances (i.e. CSM scenario 2) provides the best results and offers enhanced capacity predictions, particularly for stocky cross-sections.

References

[1] Gardner, L. (2008). The continuous strength method. Proceedings of the Institution of Civil Engineers-Structures and Buildings. 161(3), 127-133.

[2] Liew, A. and Gardner, L. (2015). Ultimate capacity of structural steel cross-sections under compression, bending and combined loading. Structures. 1, 2-11.

[3] Gardner, L., Wang, F. and Liew, A. (2011). Influence of strain hardening on the behavior and design of steel structures. International Journal of Structural Stability and Dynamics. 11(5), 855-875.

[4] Saliba, N. and Gardner, L. (2013). Cross-section stability of lean duplex stainless steel welded I-sections. Journal of Constructional Steel Research. 80, 1-14.

[5] Saliba, N. (2012). Structural behaviour of lean duplex stainless steel welded I-sections. PhD thesis. Department of Civil and Environmental Engineering, Imperial College London, UK.

[6] Afshan, S. and Gardner, L. (2013). The continuous strength method for structural stainless steel design. Thin-Walled Structures. 68, 42-49.

[7] Saliba, N. and Gardner, L. (2013). Experimental study of the shear response of lean duplex stainless steel plate girders. Engineering Structures. 46, 375-391.

[8] Saliba, N., Real, E. and Gardner, L. (2014). Shear design recommendations for stainless steel plate girders. Engineering Structures. 59, 220-228.

[9] EN 1993-1-4: 2006+A1:2015. (2015). Eurocode 3: design of steel structures – Part 1.4: general rules – supplementary rules for stainless steels, including amendment A1 (2015). Brussels. CEN.

[10] Bleich, F. (1952). Buckling strength of metal structures. McGraw Hill. New York, USA.

[11] Basler, K., Yen, B.T., Mueller, J.A. and Thürlimann. B. (1960). Web buckling tests on welded plate girders. Welded plate girders. Bulletin no 64.

[12] Basler, K. (1961). Strength of plate girders under combined bending and shear. Proceedings of the American Society of Civil Engineers. 87(ST7), Reprint No. 187 (210), (61-14).

[13] Calladine, C.R. (1973). A plastic theory for collapse of plate girders under combined shear force and bending moment. The Structural Engineer. 51(4), 147–54.

[14] Porter, D.M., Rockey, KC. and Evans, H.R. (1975). The collapse behaviour of plate girders loaded in shear. The Structural Engineer. 53(8), 313–25.

[15] Rockey, K.C., Evans, H.R. and Porter, D.M. (1978). A design method for predicting the collapse behaviour of plate girders. Proceeding of the Institution of Civil Engineers. 2(65), 85–112.

[16] Rockey, K.C. and Skaloud, M. (1972). The ultimate load behaviour of plated girders loaded in shear. The Structural Engineer. 50(1), 29–47.

[17] ENV 1993-1-1. (1992). Eurocode 3: design of steel structures – Part 1.1: general rules and rules for buildings. CEN.

[18] Dubas, P. (1980). Reflexions sur certains problems de seurite et stabilite en cnstruction metallique. Memoires CERES (55). Liege, Belgium.

[19] Höglund, T. (1998). Shear buckling resistance of steel and aluminium plate girders. Thin-Walled Structures. 29(1–4), 13–30.

[20] Davies, A.W. and Griffith, D.S.C. (1999). Shear strength of steel plate girders. Proceedings of the Institution of Civil Engineers Structures and Buildings. 134, 147–157.

[21] Presta, F., Hendy, C.R. and Turco, E. (2008). Numerical validation of simplified theories for design rules of transversely stiffened plate girders. The Structural Engineer. 86(21), 37–46.

[22] EN 1993-1-5. (2006). Eurocode 3: Design of steel structures - Part 1.5: Plated structural elements. CEN.

[23] Höglund, T. (1971). Behaviour and strength of the web of thin plate I-girders. Bulletin no 93. Division of building statics and structural engineering. The Royal Institute of Technology, Stockholm, Sweden.

[24] Höglund, T. (1973). Design of thin plate I girders in shear and bending with special reference to web buckling. Bulletin no 94. Division of building statics and structural engineering. Royal Institute of Technology, Stockholm, Sweden.

[25] La Boube, R.A. and Yu, W.W. (1978). Cold-formed steel web elements under combined bending and shear. Proceedings of the fourth international specialty conference on cold-formed steel structures. University of Missouri-Rolla, St Louis, Missouri, USA.

[26] Evans, H.R. (1983). Longitudinally and transversely reinforced plate girders. Plated structures, stability and strength. London, UK: Applied Science Publishers.

[27] Sinur, F. and Beg, D. (2013). Moment-shear interaction of stiffened plate girders – Tests and numerical model verification. Journal of Constructional Steel Research. 85, 116–129.

[28] Sinur, F. and Beg, D. (2013). Moment-shear interaction of stiffened plate girders – numerical study and reliability analysis. Journal of Constructional Steel Research. 88, 231–243.

[29] Reis, A., Lopes, N. and Real, P.V. (2016). Shear–bending interaction in steel plate girders subjected to elevated temperatures. Thin-Walled Structures. 104, 34–43.

[30] ENV 1993-1-4. (1996) Eurocode 3: design of steel structures – part 1.4: general rules – supplementary rules for stainless steels. CEN.

[31] Carvalho, E.C.G., Van den Berg, G.J. and Van der Merwe P. (1990). Local shear buckling in cold-formed stainless steel beam webs. Proceedings of the annual technical session of the structural stability research council.

[32] Olsson, A. (2001). Stainless steel plasticity-material modelling and structural applications. PhD thesis. Lulea University of Technology. Sweden.

[33] EN 1993-1-4. (2006). Eurocode 3: Design of steel structures - Part 1.4: General rules - Supplementary rules for stainless steel. CEN.

[34] Real, E., Mirambell, E. and Estrada, I. (2007). Shear response of stainless steel plate girders. Engineering Structures. 29(7), 1626–1640.

[35] Estrada, I., Real, E. and Mirambell, E. (2007). General behaviour and effect of rigid and non-rigid end post in stainless steel plate girders loaded in shear. Part II: Extended numerical study and design proposal. Journal of Constructional Steel Research. 63(7), 985-996.

[36] Estrada, I., Real, E. and Mirambell, E. (2007b). General behaviour and effect of rigid and non-rigid end post in stainless steel plate girders loaded in shear. Part I: Experimental study. Journal of Constructional Steel Research. 63(7), 970-984.

[37] Gardner, L. and Nethercot, D.A. (2004). Numerical modeling of stainless steel structural components-A consistent approach. Journal of Structural Engineering, ASCE. 130(10), 1586-1601.

[38] Gardner, L. and Ashraf, M. (2006). Structural design for non-linear metallic materials. Engineering Structures. 28(6), 926-934.

[39] Su, M. N., Young, B. and Gardner, L. (2014). Deformation-based design of aluminium alloy beams. Engineering Structures. 80, 339-349.

[40] Ashraf, M. and Young, B. (2011). Design formulations for non-welded and welded aluminium columns using Continuous Strength Method. Engineering Structures. 33(12), 3197-3207.

[41] Zhao, O., Afshan, S. and Gardner, L. (2017). Structural response and continuous strength method design of slender stainless steel cross-sections. Engineering Structures. 140, 14-25.

[42] Schafer, B.W. and Peköz, T. (1998). Computational modelling of cold-formed steel: characterizing geometric imperfections and residual stresses. Journal of Constructional Steel Research 47(3), 193-210.

[43] Hibbitt, Karlsson & Sorensen, Inc. (2010). ABAQUS. ABAQUS/Standard user's manual volumes I-III and ABAQUS CAE manual. Version 6.12. (Pawtucket, USA).

[44] Kucukler, M., Gardner, L. and Macorini, L. (2015). Lateral-torsional buckling assessment of steel beams through a stiffness reduction method. Journal of Constructional Steel Research. 109, 87-100.

[45] Theofanous, M., Chan, T.M. and Gardner, L. (2009). Flexural behaviour of stainless steel oval hollow sections. Thin-Walled Structures. 47(6-7), 776-787.

[46] Arrayago, I., Real, E. and Gardner, L. (2015). Description of stress-strain curves for stainless steel alloys. Materials and Design. 87, 540-552.

[47] Ramberg, W. and Osgood, W. R. (1943). Description of stress-strain curves by three parameters. Technical Note No 902, National Advisory Committee for Aeronautics Washington, D.C.

[48] Dawson, R.G. and Walker, A.C. (1972). Post-buckling of geometrically imperfect plates. Journal of the Structural Division, ASCE. 98(1), 75-94.

[49] Pham, C.H. and Hancock, G.J. (2012). Direct strength design of cold-formed C-sections for shear and combined actions. Journal of Structural Engineering ASCE. 138(6), 759–768.

[50] Pham, C.H., Davis, A.F. and Emmett, B.R. (2014). Numerical investigation of cold-formed lapped Z purlins under combined bending and shear. Journal of Constructional Steel Research. 95, 116–125.

[51] The MathWorks, Inc. (2012). MATLAB R2012a. Computer software, Natick, Massachusetts, USA.

Highlights

- Review of continuous strength method (CSM) design for cross-sections under normal stresses
- Derivation of CSM base curve and material model for cross-sections in shear
- Proposals for CSM shear resistance expressions
- Comparison of test and numerical data with CSM and Eurocode 3 resistance predictions

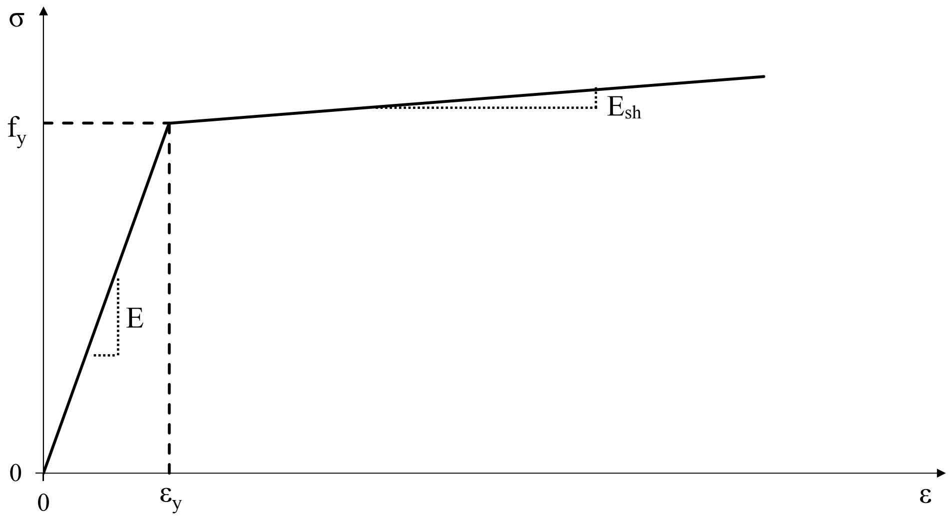

Fig. 1: Bi-linear elastic, linear hardening stress-strain model.

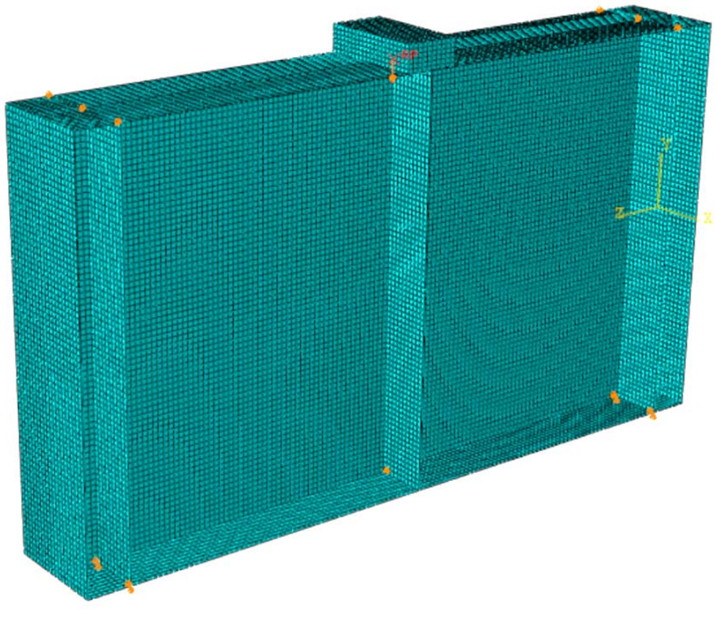

Fig. 2: Typical FE model depicting mesh, load and boundary conditions.

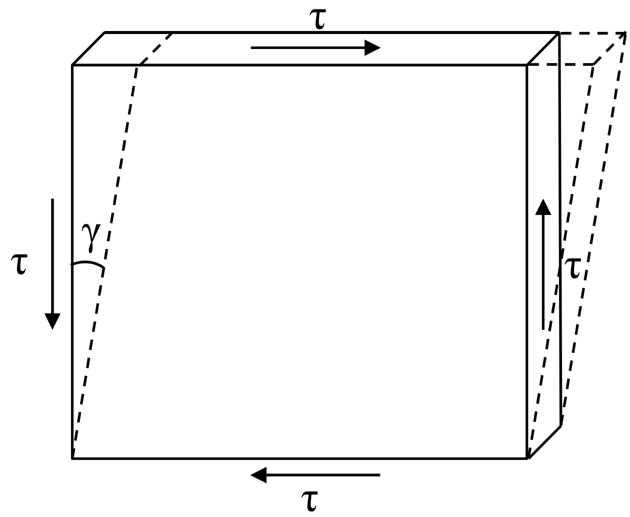

Fig. 3: Shear strain γ in a rectangular element subjected to uniform shear stress τ.

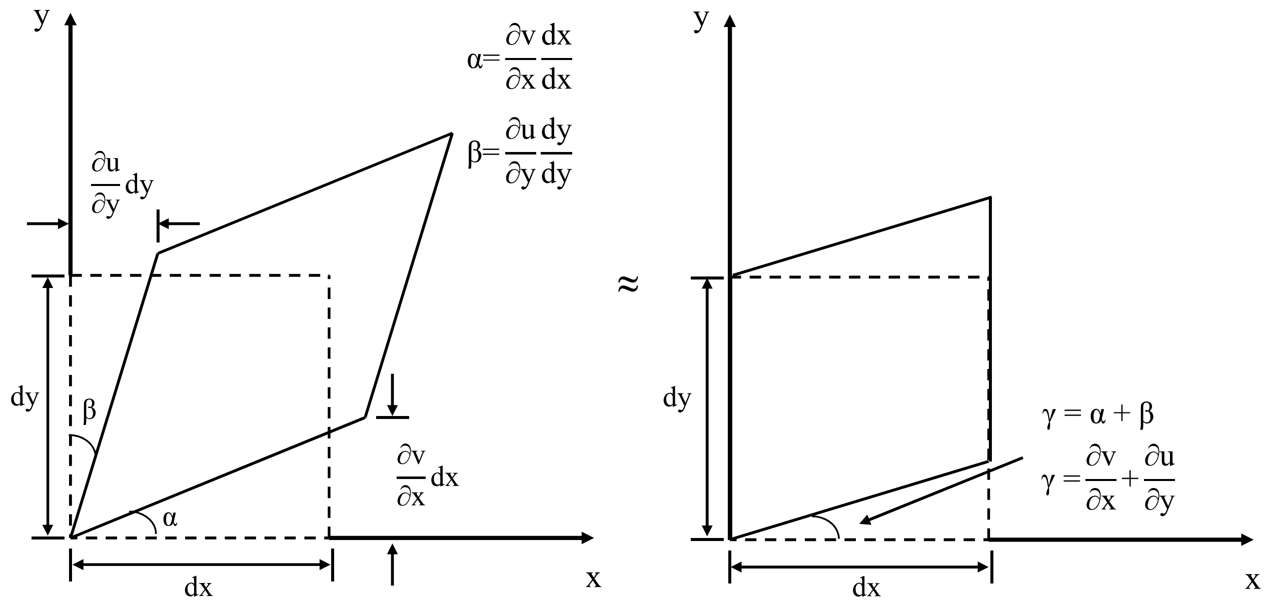

Fig. 4: Geometric deformation of an infinitesimal element and definition of the engineering shear strain γ.

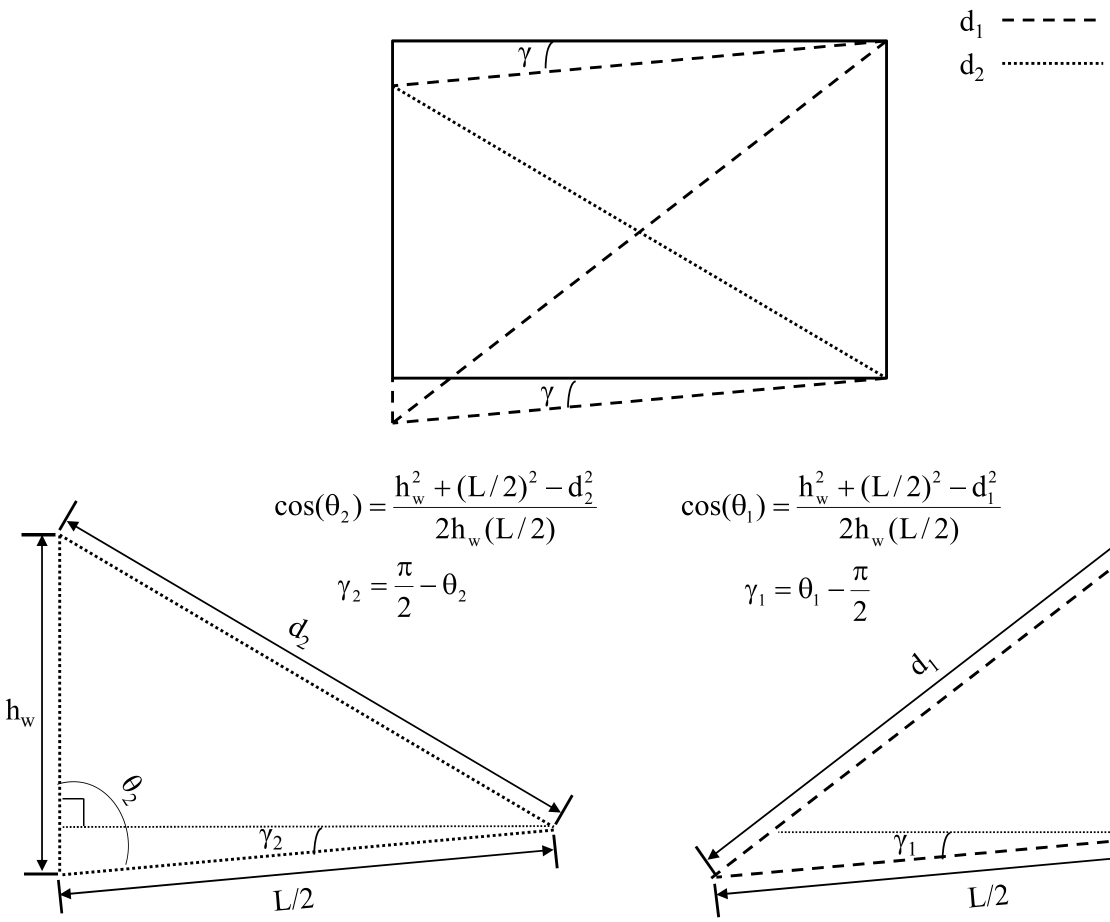

Fig. 5: Calculation of shear strain γ for the test and FE data using the diagonal readings d_1 and d_2.

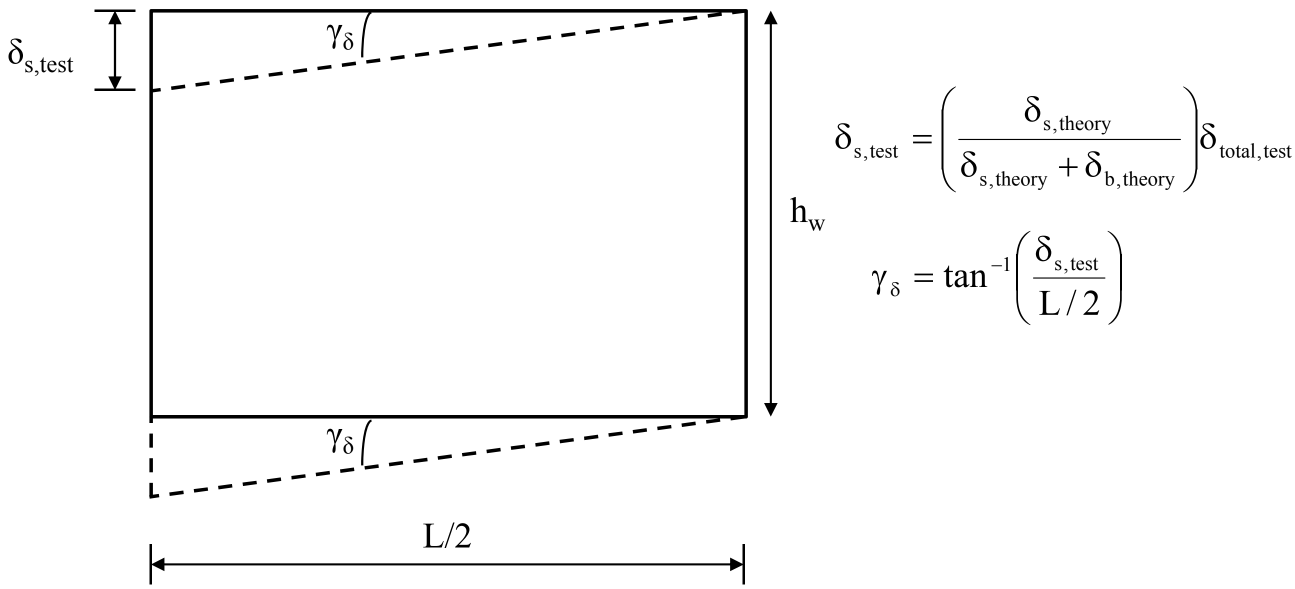

Fig. 6: Calculation of shear strain γ_δ from published results using the reported total vertical deflection $\delta_{total,test}$, modified as shown to determine $\delta_{s,test}$.

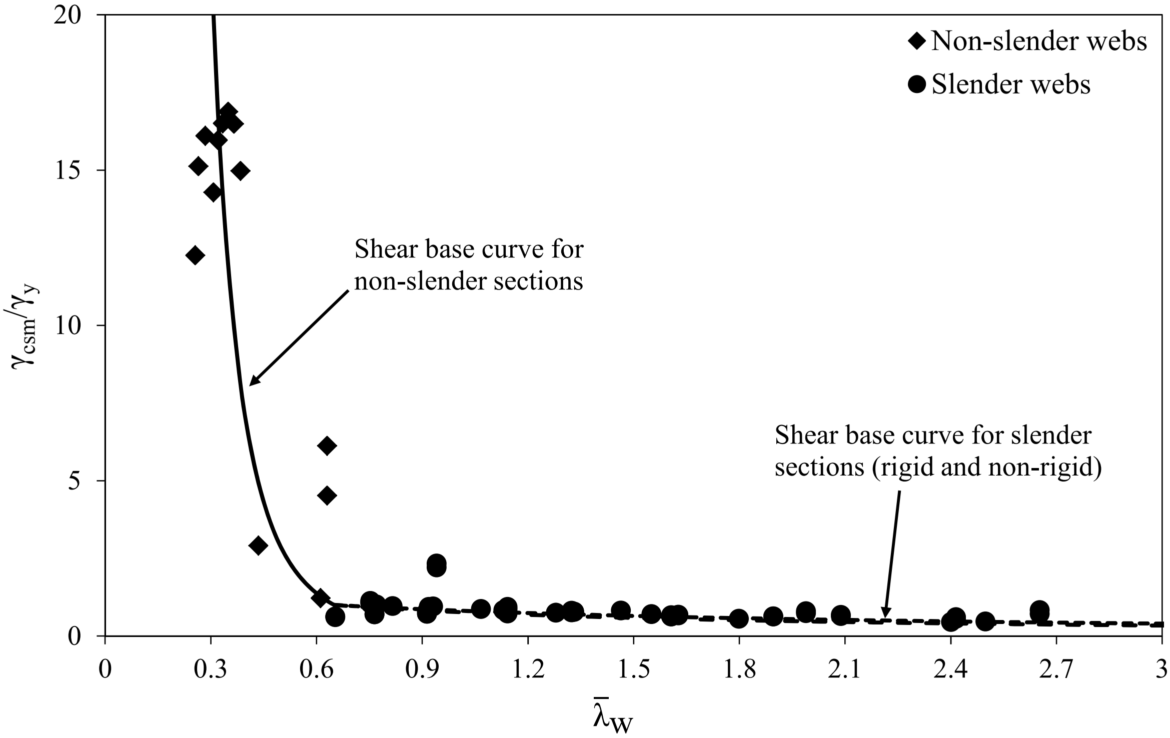

Fig. 7: Shear base curve – relationship between shear strain ratio and web slenderness.

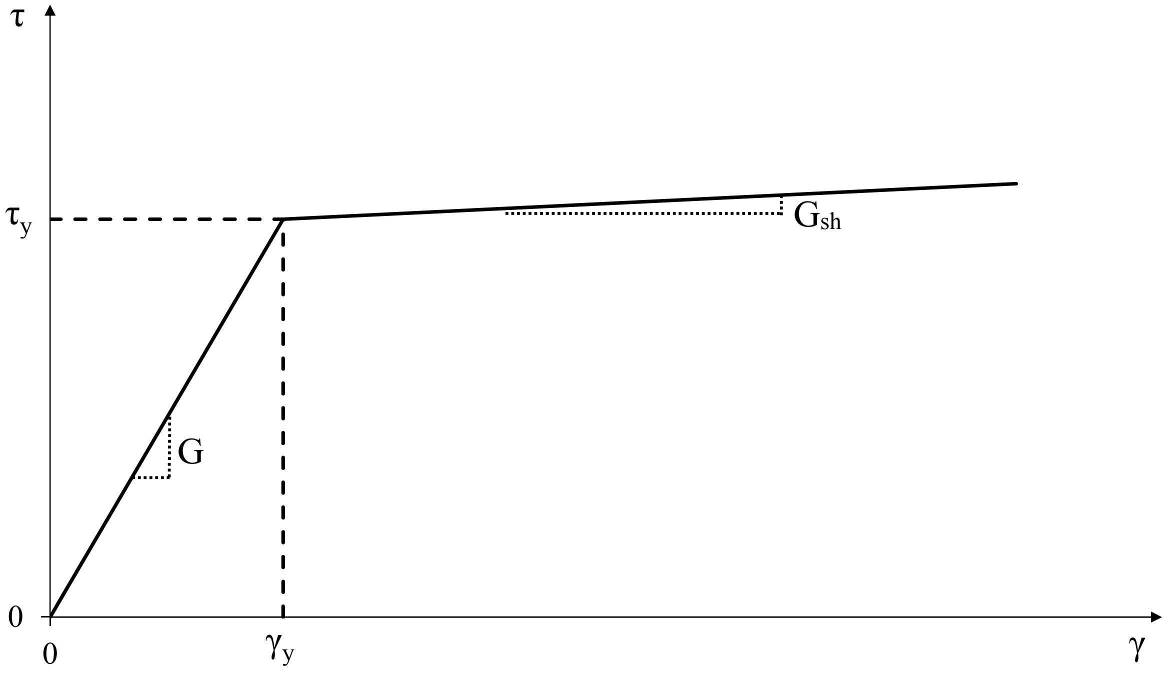

Fig. 8: Bi-linear elastic, linear hardening shear stress-strain model.

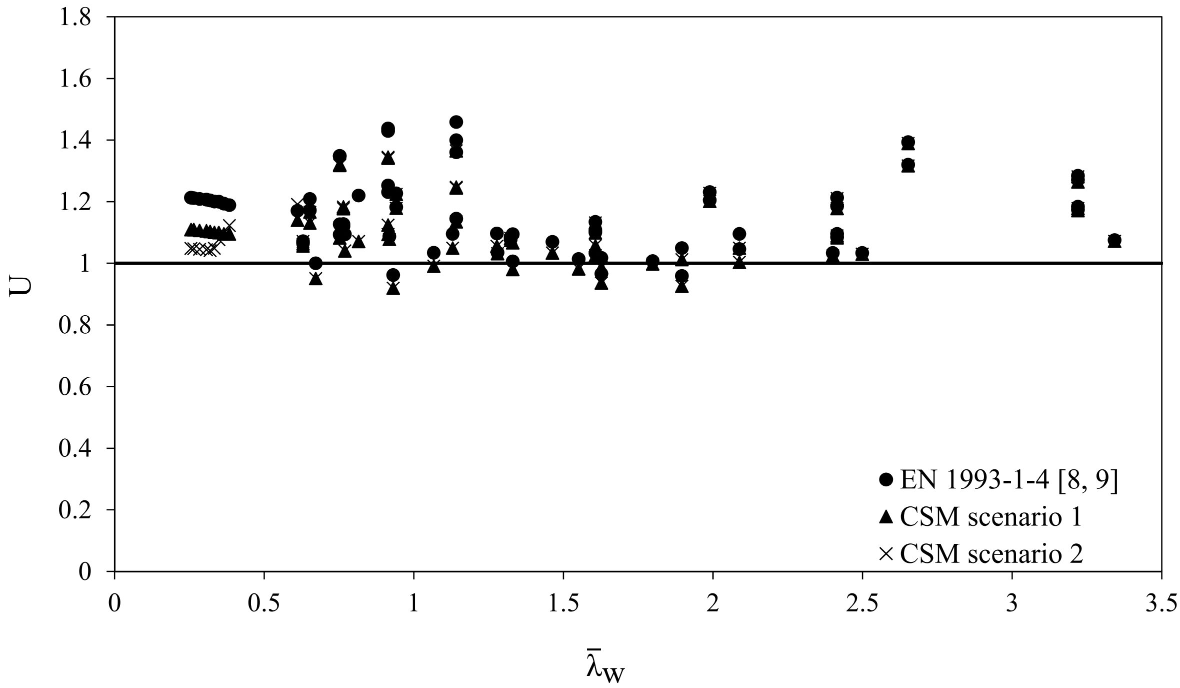

Fig. 9: Comparison of the CSM scenario 1, CSM scenario 2 and EN1993-1-4 [8, 9] with plate girder test and FE results.

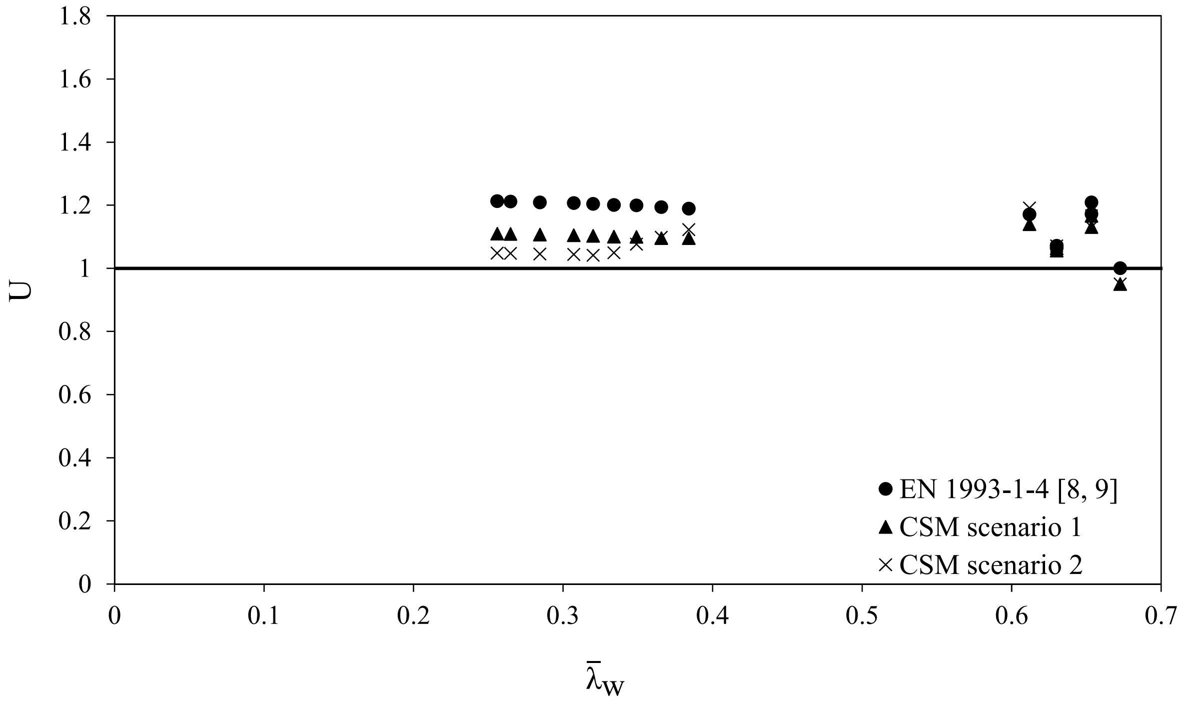

Fig. 10: Comparison of the CSM scenario 1, CSM scenario 2 and EN1993-1-4 [8, 9] with plate girder test and FE results for web slenderness $\bar{\lambda}_w < 0.65$.

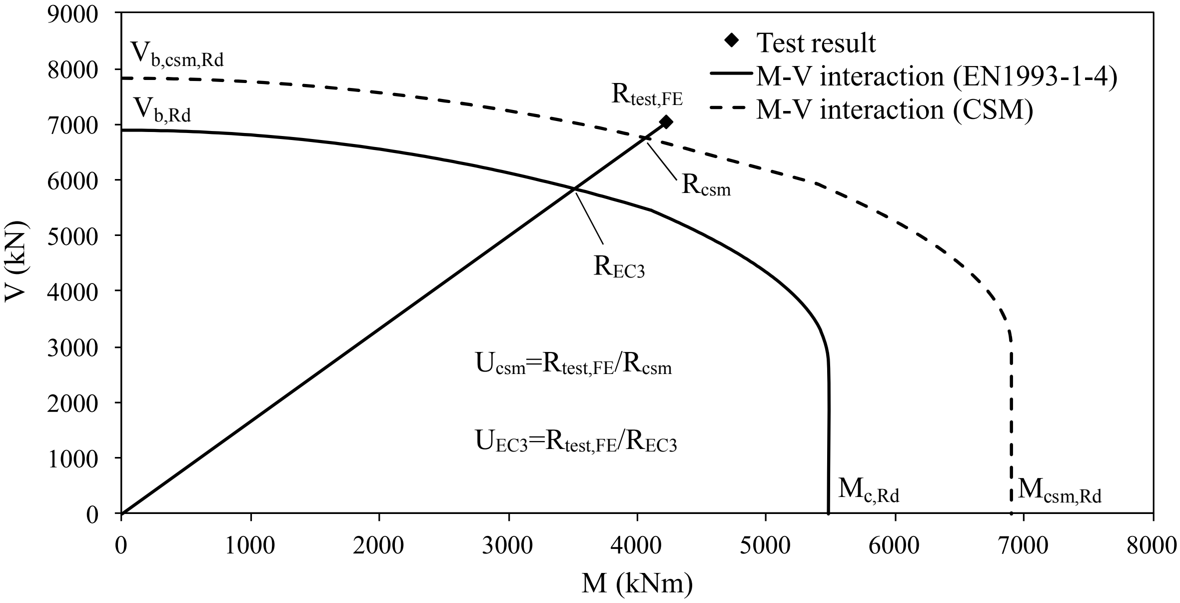

Fig. 11: Moment-shear interaction diagrams according to EN 1993-1-4 [8, 9] and CSM for plate girder I-700×200×60×25-0.86 [7].

Table 1: Web shear buckling reduction factor χ_w

	χ_w for rigid end post	χ_w for non-rigid end post
$\bar{\lambda}_w \leq 0.65/\eta$	η	η
$0.65/\eta < \bar{\lambda}_w < 0.65$	$0.65/\bar{\lambda}_w$	$0.65/\bar{\lambda}_w$
$\bar{\lambda}_w \geq 0.65$	$1.56/(0.91+\bar{\lambda}_w)$	$1.19/(0.54+\bar{\lambda}_w)$

Table 2: Summary of plate girder geometries modelled in parametric study

Plate girder designation	L (mm)	a (mm)	h_w (mm)	b_f (mm)	t_f (mm)	t_w (mm)	a/h_w
I-700×200×60×20-0.86-r	1360	600	700	200	60	20	0.86
I-700×200×60×21-0.86-r	1360	600	700	200	60	21	0.86
I-700×200×60×22-0.86-r	1360	600	700	200	60	22	0.86
I-700×200×60×23-0.86-r	1360	600	700	200	60	23	0.86
I-700×200×60×24-0.86-r	1360	600	700	200	60	24	0.86
I-700×200×60×25-0.86-r	1360	600	700	200	60	25	0.86
I-700×200× 60×27-0.86-r	1360	600	700	200	60	27	0.86
I-700×200×60×29-0.86-r	1360	600	700	200	60	29	0.86
I-700×200×60×30-0.86-r	1360	600	700	200	60	30	0.86
I- 600×200×12×2-1-r	1360	600	600	200	12	2	1.00
I-600×200×12×2-1-nr	1360	600	600	200	12	2	1.00
I-600×200×12×3-1-r	1360	600	600	200	12	3	1.00
I-600×200×12×3-1-nr	1360	600	600	200	12	3	1.00
I-600×200×12×4-1-nr	1360	600	600	200	12	4	1.00
I-600×200×12×6-1-nr	1360	600	600	200	12	6	1.00
I-600×200×12×8-1-nr	1360	600	600	200	12	8	1.00
I-600×200×12×10-1-nr	1360	600	600	200	12	10	1.00
I-600×200×15×10-1-r	1360	600	600	200	15	10	1.00
I-600×200×15×10-1-nr	1360	600	600	200	15	10	1.00
I-600×200×15×12-1-r	1360	600	600	200	15	12	1.00
I-600×200×15×12-1-nr	1360	600	600	200	15	12	1.00
I-600×200×12×2-2-r	2560	1200	600	200	12	2	2.00
I-600×200×12×2-2-nr	2560	1200	600	200	12	2	2.00
I-600×200×12×3-2-r	2560	1200	600	200	12	3	2.00
I-600×200×12×3-2-nr	2560	1200	600	200	12	3	2.00
I-600×200×12×4-2-nr	2560	1200	600	200	12	4	2.00
I-600×200×12×6-2-nr	2560	1200	600	200	12	6	2.00
I-600×200×12×8-2-nr	2560	1200	600	200	12	8	2.00
I-600×200×12×10-2-nr	2560	1200	600	200	12	10	2.00
I-600×200×15×2-2-r	2560	1200	600	200	15	2	2.00
I-600×200×15×2-2-nr	2560	1200	600	200	15	2	2.00
I-600×200×15×3-2-r	2560	1200	600	200	15	3	2.00
I-600×200×15×3-2-nr	2560	1200	600	200	15	3	2.00
I-600×200×15×4-2-r	2560	1200	600	200	15	4	2.00
I-600×200×15×4-2-nr	2560	1200	600	200	15	4	2.00
I-600×200×15×6-2-r	2560	1200	600	200	15	6	2.00
I-600×200×15×6-2-nr	2560	1200	600	200	15	6	2.00
I-600×200×15×8-2-r	2560	1200	600	200	15	8	2.00
I-600×200×15×8-2-nr	2560	1200	600	200	15	8	2.00
I-600×200×15×10-2-r	2560	1200	600	200	15	10	2.00
I-600×200×15×10-2-nr	2560	1200	600	200	15	10	2.00
I-600×200×15×12-2-r	2560	1200	600	200	15	12	2.00
I-600×200×15×12-2-nr	2560	1200	600	200	15	12	2.00
I-600×200×15×15-2-nr	2560	1200	600	200	15	15	2.00

Table 3: Comparison of CSM scenario 1, CSM scenario 2 and EN 1993-1-4 [8, 9] resistance predictions with plate girder test and FE results

No. of tests and FE models: 71	$U_{EC3\ [8,9]}$	$U_{csm,scenario\ 1}$	$U_{csm,scenario\ 2}$
Shear resistance	$V_{bw,Rd,EC3} + V_{bf,Rd,EC3}$	$V_{bw,Rd,EC3} + V_{bf,csm,Rd}$	$V_{bw,csm,Rd} + V_{bf,csm,Rd}$
Bending resistance	$M_{y,c,Rd}$	$M_{y,c,csm,Rd}$	$M_{y,c,csm,Rd}$
Mean	1.16	1.12	1.11
COV	0.10	0.10	0.10

Table 4: Comparison of CSM scenario 1, CSM scenario 2 and EN 1993-1-4 [8, 9] resistance predictions with plate girder test and FE results for web slenderness $\bar{\lambda}_w < 0.65$

No. of tests and FE models: 13	$U_{EC3\ [8,9]}$	$U_{CSM\ scenario\ 1}$	$U_{CSM\ scenario\ 2}$
Shear resistance	$V_{bw,Rd,EC3} + V_{bf,Rd,EC3}$	$V_{bw,Rd,EC3} + V_{bf,csm,Rd}$	$V_{bw,csm,Rd} + V_{bf,csm,Rd}$
Bending resistance	$M_{y,c,Rd}$	$M_{y,c,csm,Rd}$	$M_{y,c,csm,Rd}$
Mean	1.18	1.10	1.07
COV	0.04	0.02	0.04